

BOUNDARY NODE CORRECTION AND SUPERCONVERGENCE IN THE FEM

M. YAO AND D. S. MALKUS*

Department of Engineering Mechanics, University of Wisconsin–Madison, Madison, WI 53706, U.S.A.

SUMMARY

Convergence improvement and superconvergence behaviour, obtained by the simple boundary node correction (BNC) procedure for certain stress-like variables of smoothed FEM solutions, are reported in this paper. The effectiveness of BNC is shown through three examples of steady flow problems, and a posterior error analysis based on the multiple-mesh extrapolation technique has been used for estimating the convergence rates.

KEY WORDS Boundary node correction Pressure smoothing Finite element method Superconvergence
Posterior error analysis Multiple mesh extrapolation

1. INTRODUCTION

In the Galerkin/penalty finite element formulation with the reduced and selective integration technique, or in the mixed FEM with the discontinuous pressure approximation, the pressure field is expected to have jumps from element to element. As a matter of fact, all velocity (or displacement) derivatives for C^0 -isoparametric elements are, in general, discontinuous across element boundaries. Thus for post-processing purposes it is desirable to employ a smoothing scheme to smooth the solutions. Another reason for employing a smoothing procedure is that certain FE elements, such as the bilinear/constant- p , have ‘spurious pressure modes’.¹ Although these modes are automatically ‘filtered’ by using the penalty formulation, the associated generalized checkerboard modes² are often present, particularly in problems with singularities.¹ In such cases, filtering or smoothing of the pressure is required. In practice, the smoothing scheme is applicable not only to pressure but also to stress and stress-like variables. Usually, smoothing schemes of a least-squares type^{1,3} seem to perform very well at interior nodes but leave something to be desired at boundary nodes. To improve upon the results, a ‘correction’ at each boundary node can be performed.^{4,5} Even when no generalized checkerboards are present, smoothing of the stress-like variables can lead to improved accuracy.

In this paper we would like to share our experience of applying *boundary node correction* (BNC) on the smoothed field solutions and to report some convergence improvement for certain stress-like variables at the boundary which we have observed in our flow problem solving. The convergence improvement and superconvergence behaviour achieved through BNC will be shown via three examples of flow problems with a posterior error analysis⁶ based on multi-mesh extrapolation.

* Also at The Center for the Mathematical Sciences, University of Wisconsin–Madison, Madison, Wisconsin, U.S.A.

2. BOUNDARY NODE CORRECTION

Consider the standard four-node isoparametric element. The smoothed values at internal nodes are usually good and need no correction. The boundary nodes can be further segregated into three groups, i.e. non-corner boundary nodes, external corner nodes and internal corner nodes, as illustrated in Figure 1. BNC can be formulated in the physical co-ordinate system or in the isoparametric mapped co-ordinate system. In our numerical computation BNC is carried out in the following steps *in order*.^{4,5}

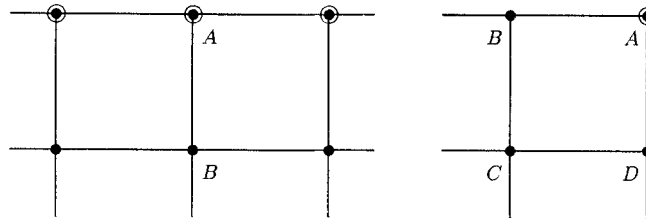
1. Correct *non-corner boundary nodes* by the linear extrapolation

$$\tilde{P}_A \leftarrow 2P_A - P_B, \quad (1)$$

where A is a typical non-corner boundary node, B is the adjacent internal node on the same element side (see Figure 1(a)), P is the smoothed pressure and \tilde{P} is the corrected P .

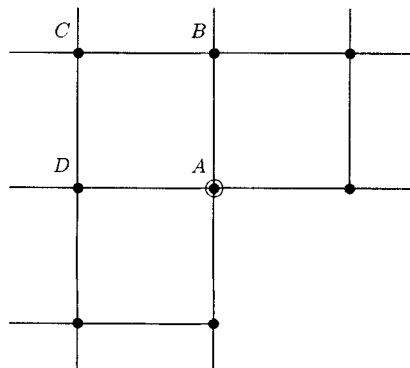
2. Correct *external corner nodes* by either the physical co-ordinate formulation

$$\tilde{P}_A \leftarrow (\tilde{L}_B P_B + \tilde{L}_C P_C + \tilde{L}_D P_D)/L, \quad (2)$$



(a) Noncorner Boundary Node

(b) External Corner Node



(c) Internal Corner Node

Figure 1. Definition of three types of boundary nodes

where

$$\tilde{L}_B = L_B + (x_{2C} - x_{2D})x_{1A} + (x_{1D} - x_{1C})x_{2A}, \quad (3a)$$

$$\tilde{L}_C = L_C + (x_{2D} - x_{2B})x_{1A} + (x_{1B} - x_{1D})x_{2A}, \quad (3b)$$

$$\tilde{L}_D = L_D + (x_{2B} - x_{2C})x_{1A} + (x_{1C} - x_{1B})x_{2A}, \quad (3c)$$

$$L_B = x_{1C}x_{2D} - x_{1D}x_{2C}, \quad (4a)$$

$$L_C = x_{1D}x_{2B} - x_{1B}x_{2D}, \quad (4b)$$

$$L_D = x_{1B}x_{2C} - x_{1C}x_{2B}, \quad (4c)$$

$$L = L_B + L_C + L_D, \quad (5)$$

or the isoparametric mapped co-ordinate formulation

$$\tilde{P}_A = P_B - P_C + P_D. \quad (6)$$

Here A, B, C and D are the four nodes of the corner element, with A being the external corner node as shown in Figure 1(b).

3. Correct *internal corner nodes* (see Figure 1(c)) by the same linear extrapolation through nodes B, C and D using (2)–(5) or (6).

It should be emphasized that the order of BNC steps is of great importance and ought to be followed exactly, because for an external corner element there are three nodes that need corrections and the corner node correction obviously depends upon the other two non-corner boundary nodes, which should be corrected first.

From equations (1)–(6) we can see that the BNC formulae, and hence the BNC results, of the formulations in both physical co-ordinates and isoparametric mapped co-ordinates are exactly the same at non-corner boundary nodes. At corner nodes it is easy to verify that equations (2)–(5) are equivalent to (6) for rectangular elements. Therefore the real difference between the two formulations will emerge only for non-rectangular elements. Obviously, equation (6) is computationally much simpler since no explicit evaluation of co-ordinates is needed.

3. NUMERICAL RESULTS

The FEM program FLUCODE⁷ which we have used in our numerical computations employs the Galerkin/penalty formulation and the NRC element,¹ which is a quadrilateral formed by four linear triangles whose interior sides define the diagonals of the quadrilateral. The velocity is approximated by a linear function and the stress and pressure are approximated by piecewise constants on each triangular element. The pressure-smoothing scheme of Malkus–Olsen¹ is implemented for post-processing of pressure, stress and other stress-like variables, such as the shear strain rate $\dot{\gamma}$ and the first normal stress difference N_1 . The BNC procedure is as described in Section 2. FLUCODE can be used for solving flow problems of some non-Newtonian fluids as well as Newtonian fluids. For non-Newtonian flows, FLUCODE is implemented with the single-integral form model and the particle-tracking technique.¹

The first example is a Stokes flow over a transverse slot ($Re = 0$). The co-ordinate system, FE mesh and boundary conditions are shown in Figure 2. The pressure at the flow outlet before and after BNC is plotted in Figure 3. This is a typical example for illustrating the importance of following the order of BNC steps. One can see from Figure 3 that the good result (plotted as solid line) is obtained only by following the order of BNC steps exactly.

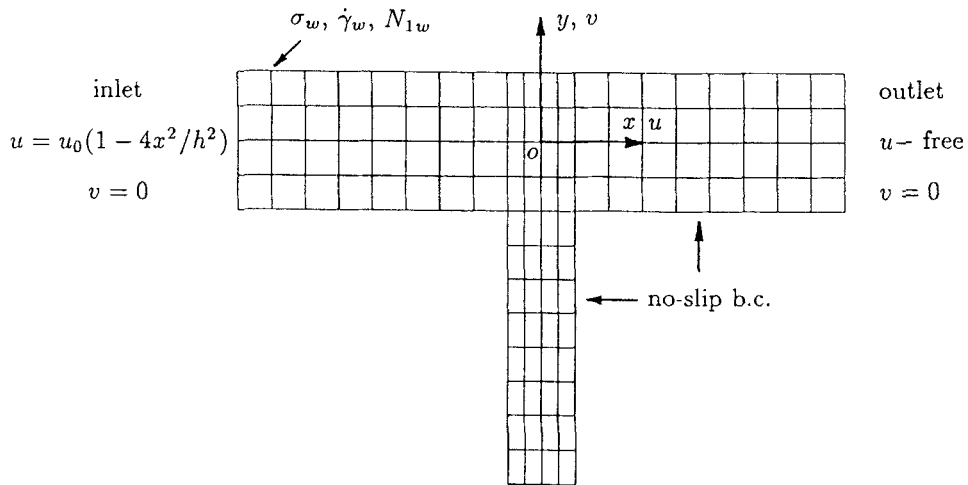


Figure 2. 2D flows over a transverse slot

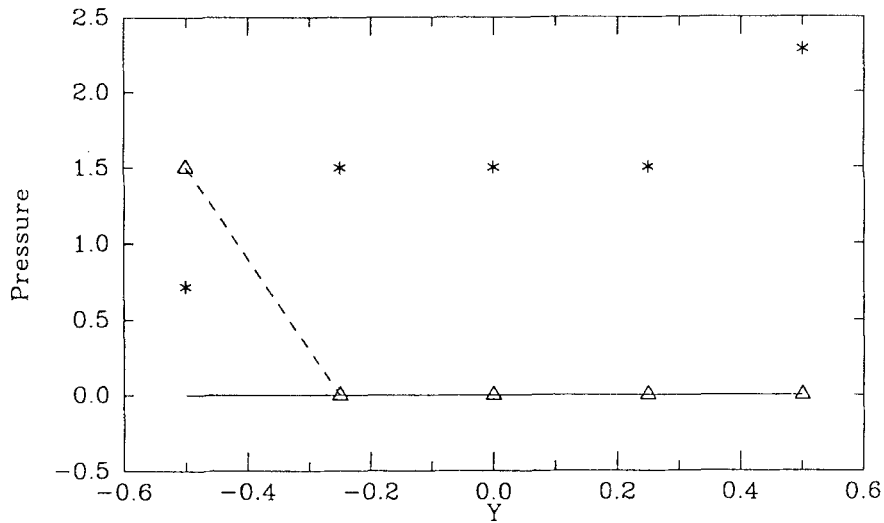


Figure 3. Pressure BNC at flow outlet for example 1: *, smoothed pressure before BNC; Δ , corrected pressure when BNC is carried out in order of FE nodal numbering; —, corrected pressure by following exactly the order of BNC steps given in Section 2

The second example is a planar Poiseuille flow over a transverse slot of a Maxwell fluid. We use this flow problem to show the superconvergence behaviour of certain quantities achieved by BNC. The posterior error analysis and multiple-mesh extrapolation technique⁶ were used to estimate the convergence rate (see the Appendix for a brief review). The FE mesh 1 and boundary conditions are the same as shown in Figure 2, except that outlet velocity profile is also specified in this case. The subsequent meshes obtained by subdividing mesh 1 are described in the Appendix. The material parameters we used are: relaxation time $T = 0.9666$; zero-shear-rate viscosity $\mu(0) = 4101.25$; slip parameter $a = 1$. Table I shows the superconvergence of the undisturbed wall

Table I. Superconvergence of S and $\dot{\gamma}_w$ achieved by BNC(a) Raw and extrapolated S by meshes 1, 2, 3 before BNC

De	Δx_1	Δx_2	Δx_3	L_{12}	L_{23}	Q_{123}	C_1	C_2	r_1	r_2
0.10	0.07500	0.08750	0.09167	0.1000	0.1000	0.1000	-0.1003	0.0010	-0.002	3.0
0.25	0.18750	0.21875	0.22917	0.2500	0.2500	0.2500	-0.2500	0.0000	0.000	3.0
0.50	0.37500	0.43750	0.45834	0.5000	0.5000	0.5002	-0.5002	0.0000	0.000	3.0
1.00	0.75004	0.87501	0.91669	1.000	1.000	1.000	-1.001	0.0040	0.000	3.0

(b) Raw and extrapolated S by meshes 1, 2, 3 after BNC

De	Δx_1	Δx_2	Δx_3	L_{12}	L_{23}	Q_{123}	C_1	C_2
0.10	0.10000	0.10000	0.10000	0.1000	0.1000	0.1000	-0.0005	0.0010
0.25	0.25000	0.25001	0.25001	0.2500	0.2500	0.2500	-0.0003	0.0006
0.50	0.50000	0.50000	0.50000	0.5000	0.5000	0.5000	-0.0010	0.0030
1.00	1.0000	1.0000	1.0000	1.000	1.000	1.000	-0.0030	0.0095

Table II. Convergence improvement of N_{1w} by BNC(a) Raw and extrapolated N_{1w} by meshes 1, 2, 3 before BNC

De	Δx_1	Δx_2	Δx_3	L_{12}	L_{23}	Q_{123}	C_1	C_2	r_1	r_2
0.10	47.732	64.952	71.307	82.172	84.019	84.943	-171.0	88.69	-0.13	2.71
0.25	298.33	406.06	445.68	513.79	524.91	530.46	-1062.0	533.4	-0.13	2.72
0.50	1193.3	1624.2	1782.7	2055.1	2099.6	2121.9	-4249.0	2137.0	-0.13	2.72
1.00	4773.6	6496.7	7130.8	8219.8	8399.1	8488.7	-17011.0	8604.6	-0.13	2.72

(b) Raw and extrapolated N_{1w} by meshes 1, 2, 3 after BNC

De	Δx_1	Δx_2	Δx_3	L_{12}	L_{23}	Q_{123}	C_1	C_2	r_1	r_2
0.10	68.947	80.864	83.095	92.780	87.557	84.945	-1.314	-250.7	47.7	5.34
0.25	430.93	505.52	519.36	580.10	547.05	530.53	-1.785	-1586.0	222.0	5.39
0.50	1723.7	2022.0	2077.4	2320.4	2188.2	2122.2	-8.123	-6343.0	195.0	5.39
1.00	6895.4	8087.8	8309.6	9280.1	8753.4	8490.0	-57.97	-25282.0	109.0	5.37

(c) Raw and extrapolated N_{1w} by meshes 1, 2, 4 after BNC

De	Δx_1	Δx_2	Δx_4	L_{12}	L_{24}	Q_{124}	C_1	C_2	r_1	r_2
0.10	68.947	80.864	83.864	92.780	86.865	84.893	-0.6904	-252.4	91.4	3.97
0.25	430.93	505.52	524.14	580.10	542.77	530.33	0.5786	-1592.0	-688.0	4.00
0.50	1723.7	2022.0	2096.5	2320.4	2171.0	2121.2	3.658	-6374.0	-436.0	4.00
1.00	6895.4	8087.8	8386.0	9280.1	8684.3	8485.7	-6.371	-25420.0	997.0	4.00

shear rate $\dot{\gamma}_w$ and the scaled shear stress $S = T\sigma_w/\mu(0)$. S and $\dot{\gamma}_w$ have a first-order convergence rate when they are just smoothed, as shown in Table I(a). From Table I(b) one can see that they gain superconvergence after BNC, and even the crudest mesh gives the exact values of S and $\dot{\gamma}_w$ (here we have $S = T\dot{\gamma}_w \equiv De$). The convergence improvement of N_{1w} (the undisturbed first normal stress difference at the wall) is given in Table II. As indicated by the convergence indicator r_2 , the convergence rate of N_{1w} is improved from first order before BNC to second order after BNC. The exact values of N_{1w} at $De = 0.10, 0.25, 0.5$ and 1.0 are $N_{1w} = 2\mu(0)(De)^2/T \doteq 84.859$,

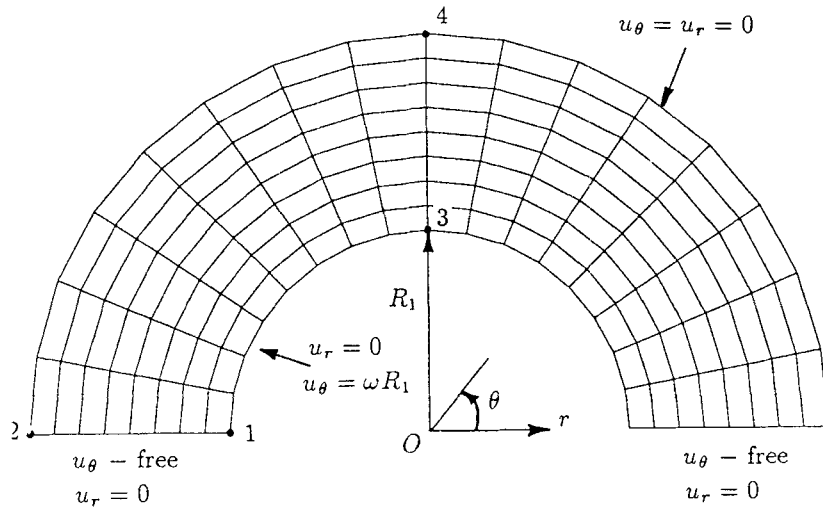


Figure 4. 2D flow between two concentric cylinders

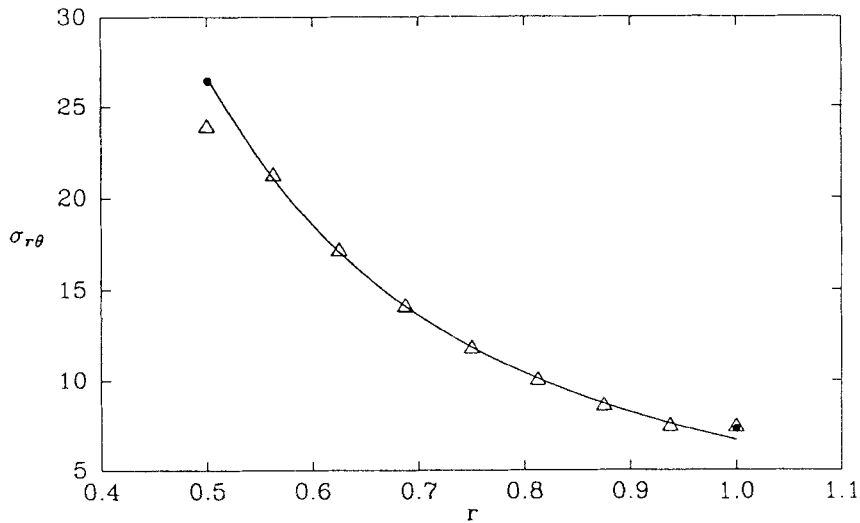


Figure 5. BNC of shear stress $\sigma_{r,\theta}$ for example 3: —, analytical solution $\sigma_{r\theta} = 20/(3r^2)$; Δ , smoothed FEM solution by FLUCODE; \bullet , BNC corrected values

530-37, 2121-5 and 8485-9 respectively. We conclude that S , $\dot{\gamma}_w$ and N_{1w} gain superconvergence because, on the basis of the linear element used in FLUCODE, we are generally expecting only a first-order convergence rate in stress-like variables.

The third example is a Stokes flow between two concentric cylinders ($Re = 0$) with the outer cylinder fixed and the inner cylinder rotating at constant angular velocity ω . We choose this problem to show how BNC works for non-rectangular elements. One of the meshes, i.e. mesh 2, with boundary conditions is pictured in Figure 4. The dimensionless parameters used are: $\omega = 10$; radius of inner cylinder, $R_1 = 0.5$; radius of outer cylinder, $R_2 = 1$; density $\rho = 0$; viscosity $\eta = 1$.

Table III. Raw and extrapolated $\sigma_{r\theta}$ by meshes 1, 2, 4 after BNC

Node	Δx_1	Δx_2	Δx_4	L_{12}	L_{24}	Q_{124}	$\sigma_{r\theta}^{\text{exact}}$
1	25.982	27.353	27.093	28.723	26.833	26.202	26.667
2	10.611	7.9585	7.2142	5.3065	6.4699	6.8578	6.6667
3	25.320	26.500	26.751	27.680	27.002	26.776	26.667
4	7.2498	7.3106	7.0704	7.3714	6.8301	6.6497	6.6667
1*	28.002	27.711	27.146	27.421	26.581	26.301	26.667
2*	9.9251	7.8833	7.2055	5.8415	6.5277	6.7565	6.6667

Figure 5 shows the BNC results for the shear stress $\sigma_{r\theta}$ along the radial direction ($\theta = \pi/2$ in Figure 4). One can see that BNC did a good job at the inner cylinder boundary (where the velocity gradient is large) but made hardly any improvement at the outer cylinder boundary (where the velocity gradient is small). The three-mesh (meshes 1, 2 and 4) extrapolation results for the shear stress at some boundary nodes are given in Table III. An improvement in convergence rate has been observed after BNC at some boundary nodes, such as 2 and 3 in Figure 4. The first four rows of Table III are computed by the physical co-ordinate formulation, namely equations (1)–(5). The last two rows of Table III, i.e. 1* and 2*, are obtained by equation (6) at corner nodes 1 and 2. The numerical results of this example show that for a crude mesh the value corrected by (6) may sometimes not be as good as that given by (2)–(5) (e.g. compare the $\sigma_{r\theta} = 28.002$ of mesh 1 in the penultimate row with $\sigma_{r\theta} = 25.982$ in the second row in Table III). However, for a fine mesh the boundary values corrected by (6) and (2)–(5) are very close; and also the accuracy of the extrapolated Q_{124} based on (6) seems a little better than those based on (2)–(5). Therefore it is hard to say which formulation is really superior in accuracy solely from this particular example.

4. CLOSING REMARKS

Our numerical experience shows that BNC is quite effective in improving the accuracy of smoothed FE solutions at the boundary and is applicable not only to pressure but also to stress and other stress-like variables. The BNC formulation in the isoparametric mapped co-ordinate system, i.e. equation (6), is seemingly preferable because of its simplicity in computation and because it yields the same results for rectangular elements and at least the same accuracy for fine-enough non-rectangular elements. Improved convergence rate and superconvergence behaviour have been observed for certain variables, such as σ_{12} , $\dot{\gamma}$ and N_1 , after BNC at the part of the boundary where the velocity (or displacement) gradient is large. However, according to our numerical results, there is no convergence improvement by BNC at non-corner boundary nodes where the velocity (or displacement) gradient is small.

APPENDIX: POSTERIOR ERROR ANALYSIS AND MULTIPLE-MESH EXTRAPOLATION⁶

Let $H(\sigma, \Delta x)$ denote a typical quantity in the FEM solution, such as the first normal stress difference $N_1(\sigma, \Delta x)$. Here $N_1(\sigma, \Delta x)$ is the value of $N_1(\sigma)$ computed by the FEM on a grid with typical element size Δx . Then $H(\sigma, \Delta x)$ is presumed to have an asymptotic error series in Δx about $\Delta x = 0$, i.e.

$$H(\sigma, \Delta x) = H(\sigma, 0) + (\Delta x)^{\nu} [C_1(H, \sigma) + C_2(H, \sigma)\Delta x + C_3(H, \sigma)(\Delta x)^2 + \dots] \quad (7)$$

for $0 < \nu \leq 1$. $C_i(H, \sigma)$ are coefficients to be determined; $\nu = 1$ is appropriate for the results presented here.⁶

The basic technique of posterior error analysis is multiple-mesh extrapolation. One can begin with a crude mesh, e.g. mesh 1 with Δx_1 . The subsequent meshes are obtained by subdividing mesh 1 equally in both co-ordinate directions. Use Δx_i to denote the typical element size of mesh i ($i = 1, 2, 3, 4$) and assume $\Delta x_2 = \Delta x_1/2$, $\Delta x_3 = \Delta x_1/3$, $\Delta x_4 = \Delta x_1/4$. Taking three-mesh extrapolation as an example, we first view (7) as the general interpolation problem with truncated finite terms, i.e.

$$C_0 + \Delta x_i C_1 + (\Delta x_i)^2 C_2 = H(\sigma, \Delta x_i) \quad (i = 1, 2, 3), \quad (8)$$

where $C_0 \doteq H(\sigma, 0)$, $C_1 \doteq C_1(H, \sigma)$ and $C_2 \doteq C_2(H, \sigma)$. Then we introduce the notation used by Malkus to write the extrapolation procedure simply in terms of the linear and quadratic extrapolation results, namely

$$\begin{aligned} L_{12}(H, \sigma) &= 2H(\sigma, \Delta x_1/2) - H(\sigma, \Delta x_1), \\ L_{23}(H, \sigma) &= 3H(\sigma, \Delta x_1/3) - 2H(\sigma, \Delta x_1/2), \\ Q_{123}(H, \sigma) &= \frac{3}{2}L_{23}(H, \sigma) - \frac{1}{2}L_{12}(H, \sigma). \end{aligned} \quad (9)$$

Here $L_{rm}(H, \sigma)$ ($r, m = 1, 2, 3, 4$) represents the linear extrapolation value of $H(\sigma, \Delta x)$ at $\Delta x = 0$, approximated by meshes r and m , and $Q_{rms}(H, \sigma)$ ($r, m, s = 1, 2, 3, 4$) denotes the quadratic extrapolation value of H at $\Delta x = 0$, approximated by meshes r, m and s . By solving (8) and using (9), one can get C_0, C_1 and C_2 in terms of L_{12}, L_{23} and Q_{123} , accurate to $O(|\Delta x_1|^3)$.

Three useful internal consistency checks are also proposed in Reference 6, two of which were used in this paper: They are:

(i) Computing

$$r_1 \equiv C_2(H, \sigma)\Delta x_1/C_1(H, \sigma) \doteq C_2\Delta x_1/C_1$$

to estimate the relative contributions at first and second order respectively

(ii) checking

$$r_2 \equiv \frac{H(\sigma, \Delta x_1) - H(\sigma, \Delta x_2)}{H(\sigma, \Delta x_2) - H(\sigma, \Delta x_3)}$$

to estimate the dominance of the leading-order term over the rest of the asymptotic series.⁸

In regard to (ii), if the discretization error $E_A(H, \sigma, \Delta x) \doteq C_i(\Delta x)^{p_i} + o(|\Delta x|^{p_i})$ and if the 'little o ' is sufficiently small, we have

$$r_2 \sim \frac{(\Delta x_1)^{p_1} - (\Delta x_2)^{p_1}}{(\Delta x_2)^{p_1} - (\Delta x_3)^{p_1}}. \quad (10)$$

When meshes 1, 2 and 3 are used, (10) yields

$$r_2(1, 2, 3) = \frac{1 - (1/2)^{p_1}}{(1/2)^{p_1} - (1/3)^{p_1}} = \begin{cases} 3.0, & p_1 = p_2 = 1, \\ 5.4, & p_1 = p_2 = 2. \end{cases} \quad (11)$$

When meshes 1, 2, and 4 are used, (10) gives

$$r_2(1, 2, 4) = \frac{1 - (1/2)^{p_1}}{(1/2)^{p_1} - (1/4)^{p_1}} = \begin{cases} 2.0, & p_1 = p_2 = 1, \\ 4.0, & p_1 = p_2 = 2. \end{cases} \quad (12)$$

For a particular three-mesh extrapolation, say meshes 1, 2 and 3, we shall consider it strong evidence that the method is first order and in its asymptotic range if r_1 is small and r_2 is near 3, and that the method is second order and in its asymptotic range if r_1 is very large and r_2 is near 5.4. Otherwise we shall conclude that the analysis is indeterminate if r_2 is close to neither 3 nor 5.4. Such a case could also possibly indicate that the method is third or higher order in Δx , which we have observed for some quantities⁷ as a consequence of superconvergence after BNC.

ACKNOWLEDGEMENTS

The authors acknowledge the support of the San Diego Supercomputer Center, the U.S. Army Research Office under Grant DAAL03-87-K-0036 and the National Science Foundation under Grant DMS-8907264.

REFERENCES

1. B. Bernstein, D. S. Malkus and E. T. Olsen, 'A finite element for incompressible plane flows of fluids with memory', *Int. j. numer. methods fluids*, **5**, 43–70 (1985).
2. R. L. Sani, P. M. Gresho, R. L. Lee, D. F. Griffiths and M. Engelman, 'The cause and cure (?) spurious pressures generated by certain FEM solutions to the incompressible Navier–Stokes equations. Part I and II', *Int. j. numer. methods fluids*, **1**, 17–43, 171–204 (1981).
3. T. J. R. Hughes, W. K. Liu and A. Brooks, 'Finite element analysis of incompressible viscous flows by the penalty function formulation', *J. Comput. Phys.*, **30**, 1–60 (1979).
4. T. J. R. Hughes, *The Finite Element Method—Linear Static and Dynamic Finite Element Analysis*, Prentice-Hall, Englewood Cliffs, NJ, 1987.
5. J. M. Leone Jr. (Lawrence Livermore National Laboratory, University of California, Livermore, CA), Private communication with D. S. Malkus, December 1987.
6. D. S. Malkus and M. F. Webster, 'On the accuracy of finite element and finite difference predictions of non-Newtonian slot pressures for a Maxwell fluid', *J. Non-Newtonian Fluid Mech.*, **25**, 93–127 (1987).
7. M. Yao, 'A numerical and analytical study of normal stresses and pressure differences in non-Newtonian creeping flows', *Ph.D. Thesis*, University of Wisconsin-Madison, Madison, WI (1989).
8. S. D. Conte and C. de Boor, *Elementary Numerical Analysis*, 2nd edn, McGraw-Hill, New York, 1972.